

IER5L is a Prognostic Biomarker in Pan-Cancer Analysis and Correlates with Immune Infiltration and Immune Molecules in Non-Small Cell Lung Cancer

Xin Chen^{1,*}, Yan-Qiu He^{1,*}, Ti-Wei Miao¹, Jie Yin², Jie Liu¹, Hong-Ping Zeng¹, Qi Zhu¹

¹Department of Integrated Traditional Chinese and Western Medicine, Zigong First People's Hospital, Zigong, People's Republic of China; ²School of Automation & Information Engineering, Sichuan University of Science & Engineering, Zigong, People's Republic of China

*These authors contributed equally to this work

Correspondence: Xin Chen, Department of Integrated Traditional Chinese and Western Medicine, Zigong First People's Hospital, Zigong, People's Republic of China, Email 4651740@qq.com

Purpose: Non-small cell lung cancer (NSCLC) accounts for the majority of lung cancer cases. Immediate early response 5 like (*IER5L*) plays crucial roles in progression and prognosis for several tumors, but its role in NSCLC remains unclear.

Patients and Methods: Gene expression and mutation profiles, DNA methylation data, and clinical information for cancers were downloaded from multiple databases. Relative expression, prognostic value, and correlation with disease progression of *IER5L* were analyzed in multiple cancers, including NSCLC. Upstream mechanisms were explored using a transcriptional network. Functional enrichment analysis, protein–protein interaction network, and gene set enrichment analysis were applied to study downstream mechanisms. Correlations of *IER5L* with immune infiltration, immune molecules, methylation status, and tumor mutation burden (TMB) were analyzed using R language. Finally, quantitative polymerase chain reaction (qPCR) and single-cell RNA sequencing (scRNA seq) analysis were performed to validate *IER5L* expression in NSCLC.

Results: Pan-cancer analysis displayed that *IER5L* expression was upregulated in multiple cancers and was associated with disease prognosis and progression, including NSCLC, which was validated using qPCR. scRNA seq analysis showed that multiple cells had increased *IER5L* expression. An *EGR1*-hsa-miR-8075-*IER5L* network was constructed for NSCLC. A total of 191 DEGs were identified between the two *IER5L* groups, which were significantly enriched in biological process of action potential, sodium ion transport, and regulation of membrane potential. Increased *IER5L* expression was primarily enriched in cell cycle, NOTCH signaling pathway, and oxidative phosphorylation pathway, and was correlated with increased regulatory T cells and neutrophils, elevated levels of immune molecules, and higher TMB.

Conclusion: Our findings show that increased *IER5L* expression was correlated with progression and prognosis in multiple cancers as well as with immune infiltration and immune molecules in NSCLC. Thus, *IER5L* is a prognostic biomarker in multiple cancers and may correlate with immunotherapeutic response in NSCLC.

Keywords: immediate early response 5 like, non-small cell lung cancer, pan-cancer, prognosis, immune infiltration

Introduction

Lung cancer is the leading cause of cancer-related deaths worldwide.¹ Based on pathological point of view, lung cancer is divided into two types: non-small cell lung cancer (NSCLC) and small cell lung cancer (SCLC),² and NSCLC accounts for more than 80% of all cases.³ Unfortunately, many NSCLCs are determined at advanced stages,⁴ thus, many of them have lost surgical opportunity. Moreover, although many therapies have been developed for lung cancer, including chemotherapy, targeted therapy, and immunotherapy, its average 5-year overall survival (OS) probability remains less than 20%.^{5–7} Thus, identification of effective biomarkers to predict prognosis and even guide therapy is important for NSCLC.

Various biomarkers for diagnosis and prognosis have been identified for NSCLC using the Gene Expression Omnibus (GEO) and The Cancer Genome Atlas (TCGA) databases, such as ADAM-like decysin-1 (*ADAMDEC1*),⁸ long non-coding *RNASEH1-AS1*,⁹ sialic acid binding Ig-like lectin 15 (*Siglec15*),¹⁰ lysine acetyltransferase 2B (*KAT2B*),¹¹ and Erb-b2 receptor tyrosine kinase 4 (*ERBB4*).¹² Moreover, many gene signatures have been constructed to predict prognosis and therapeutic response for NSCLC, such as RNA-binding proteins related signature,¹³ telomere length-related gene signature,¹⁴ ferroptosis-related long non-coding RNAs signature,¹⁵ immune microenvironment signature,¹⁶ neutrophil extracellular traps-related lncRNA signature,¹⁷ and glycolysis-related gene signature.¹⁸ However, owing to complex molecular mechanisms and disease heterogeneity in NSCLC, more biomarkers having different targets and prognostic value need to be explored.

Immediate-early response family has three different members, which is activated under different conditions.¹⁹ *IER2* is activated through activating *P38* and *JNK*, whereas *IER5* expression is increased via proteotoxic stress.¹⁹ In recent years, researchers have reported that activated immediate early response 5 like (*IER5L*) is correlated with tumorigenesis and its progression. In glioblastoma, there is increased *IER5L* expression in cancer tissues compared with control tissues.²⁰ Moreover, a growth on *IER5L* expression has been reported in metastatic colorectal cancer compared with primary cancer, and is negatively correlated with survival.²¹ However, there are few pan-cancer analyses of *IER5L* and reports on the role of *IER5L* in NSCLC, so this study aimed to perform a pan-cancer analysis of *IER5L* and evaluate its value as a prognostic biomarker and a potential immunotherapeutic target for NSCLC.

In the present study, data were downloaded from several public databases. Pan-cancer analysis of *IER5L* were first performed in terms of gene expression, prognosis, and disease progression. In NSCLC, relative expression, prognostic value, and correlation with clinical parameters were analyzed using R language. Quantitative polymerase chain reaction (qPCR) and single-cell RNA sequencing (scRNA seq) analysis were used to validate dysregulated *IER5L* expression in NSCLC. Upstream and downstream mechanisms were explored using transcriptional network that was constructed using microRNA (miRNA) and transcription factors (TFs) and functional enrichment analysis, a protein–protein interaction (PPI) network, and gene set enrichment analysis (GSEA), respectively. Methylation levels of *IER5L* and tumor mutation burden (TMB) between the two groups were analyzed using R language. Finally, correlations of *IER5L* with immune infiltration and immune molecules (inhibitors and stimulators) were analyzed using R language to evaluate its value in immunotherapy.

Methods and Materials

Data Collection and Processing

The mRNA expression data and clinical information for multiple cancers were obtained from the Gene Expression Profiling Interactive Analysis 2 (GEPIA2) database (<http://gepia2.cancer-pku.cn/#index>). Moreover, mRNA expression profiles (1037 cancer and 108 controls), methylation data (807 cancer and 71 controls), gene mutation data (1059 cancer), and clinical information (1027 cancer) were downloaded from the TCGA-GDC database (<https://portal.gdc.cancer.gov/repository>). GSE31210 (226 cancer and 20 controls) and GSE30219 (293 cancer and 14 controls) datasets were downloaded from the GEO database (<https://www.ncbi.nlm.nih.gov/gds/>). GSE31210 and GSE30219 were generated from the GPL570 [HG-U133_Plus_2] Affymetrix Human Genome U133 Plus 2.0 Array. Inclusion criteria were patients with 1) NSCLC; 2) *IER5L* mRNA expression; and 3) complete follow-up data. Therefore, 987 patients from TCGA, 226 patients from GSE31210, and 268 patients from GSE30219 were included in the current study. The clinical characteristics of patients are summarized in Table 1.

Levels of *IER5L* mRNA Expression and Its Prognostic Value in a Pan-Cancer Analysis

Levels of *IER5L* mRNA expression were estimated between cancer tissues and control tissues in 23 types of cancer and among different International Cancer Control (UICC) stages in the GEPIA2 database. Moreover, patients with each kind of cancer were divided into high or low *IER5L* expression groups based on the median *IER5L* mRNA expression, and survival analysis was performed between two *IER5L* expression groups.

Table 1 Clinical Characteristics of Patients with NSCLC from Public Databases

Clinical Characteristic	TCGA (978)	GSE31210 (226)	GSE30219 (268)
Age (years)			
≥65	590 (60.33%)	62 (0.27%)	108 (40.30%)
<65	388 (39.67%)	164 (72.57%)	159 (59.22%)
Unknown	0	0	1 (0.375)
Gender			
Male	585 (59.82%)	105 (46.46%)	226 (84.33%)
Female	393 (40.185)	121 (53.54)	42 (15.67%)
Unknown	0	0	0
T classification			
T1-T2	819 (83.74%)	226 (100%)	222 (82.84%)
T3-T4	156 (15.95%)	0	44 (16.42%)
Unknown	3 (0.31%)	0	2 (0.75%)
N classification			
N0	629 (64.31%)	/	191 (71.27%)
N1-N3	333 (34.05%)	/	75 (27.99%)
Unknown	16 (1.64%)	/	2 (0.75%)
M classification			
M0	722 (73.82%)	/	261 (97.39%)
M1	31 (3.17%)	/	4 (1.49%)
Unknown	225 (23.01%)	/	2 (0.75%)
UICC stage			
Stage I-II	772 (78.94%)	226 (100%)	/
Stage III-IV	194 (19.84%)	0	/
Unknown	12 (1.23%)	0	/

Abbreviations: NSCLC, non-small cell lung cancer; TCGA, The Cancer Genome Atlas; UICC, union for international cancer control.

Levels of *IER5L* mRNA Expression in NSCLC and Controls

Levels of *IER5L* mRNA expression in NSCLC were compared with controls in TCGA, GSE31210, and GSE30219 datasets. The diagnostic value of *IER5L* was evaluated using a receiver operating characteristic (ROC) curve.

RNA Extraction and qPCR Validation

Thirty-two lung tissues (16 NSCLC and 16 controls) were obtained from patients with NSCLC in Zigong First People's Hospital. The baseline characteristics of patients are listed in Table 2. Total RNA was first extracted from lung tissues using the E.Z.N.A. HP Total RNA Kit (Omega, GA, USA) and was then applied to synthesize cDNA using The PrimeScript™ RT reagent kit (Takara, Japan) based on the manufacturer's protocol. Finally, qPCR was performed using cDNA via iQ™ SYBR Green Supermix (Bio-Rad, USA) according to the manufacturer's instructions. Levels of *IER5L* mRNA expression were normalized using β -actin Ct value in a $2^{-\Delta\Delta Ct}$ quantification method. The qPCR primers were as follows.

Table 2 The Clinical Characteristics of Patients with NSCLC from Our Cohort

Clinical Characteristics	Patients (16)
Age, years	71.5 (68.5–76)
Male, n (%)	12 (75.00%)
Smoking status, n (%)	11 (68.75%)
UICC stage I-II, n (%)	7 (43.74%)

Abbreviations: NSCLC, non-small cell lung cancer; UICC, union for international cancer control.

IER5L-forward: 5'-AGACAAAGACTCGGCAAAGGG-3'.

IER5L-reverse: 5'-TGGTAGGCTCCTCGCTAAACA-3'.

β -actin'-forward: 5'-CCACGAAACTACCTTCAACTCC'-3'.

β -actin'-reverse: 5'-GTGATCTCCTTCTGCATCCTGT'-3'.

Single-Cell RNA Sequencing Analysis

Six single-cell RNA sequencing datasets for NSCLC were downloaded from the Tumor Immune Single-cell Hub database (TISCH, <http://tisch1.comp-genomics.org/home/>) including NSCLC_EMTAB6149, NSCLC_GSE117570, NSCLC_GSE127465, NSCLC_GSE127471, NSCLC_GSE139555, and NSCLC_GSE99254. A single-cell atlas was plotted, and *IER5L* mRNA expression was compared among different cells.

The Prognostic Value of *IER5L* and Its Correlation with Clinical Characteristics

The high or low *IER5L* expression groups were constructed using NSCLC patients based on the median *IER5L* mRNA expression. The OS probability was estimated between the two groups in TCGA, GSE31210, and GSE30219, and the DFS probability was calculated in GSE30219. Moreover, the levels of *IER5L* mRNA expression were compared between the different UICC stages in TCGA, GSE31210, and GSE30219, and were also compared between patients with relapse and patients without relapse in GSE30219. Independent prognostic factors for the NSCLC were screened using univariate and multivariate Cox regression analyses with the “survival” package in TCGA, GSE31210, and GSE30219.

Nomogram and Calibration Plots of Nomogram

A nomogram was constructed for NSCLC using independent prognostic factors screened by multivariate Cox regression analysis with the “rms” package in R language (version 4.0.2). Calibration plots of the nomogram were used to assess conformity of the nomogram-predicted with actual OS probability.

IER5L Methylation Levels and Gene Mutation Analysis

Methylation data of *IER5L* in NSCLC were obtained using Strawberry Perl (version 5.34.1). Correlation of *IER5L* methylation levels with *IER5L* mRNA expression levels was evaluated using Spearman rank correlation analysis. The “maftools” package in R language was applied to analyze gene mutation frequencies between the two groups in both LUAD and LUSC. Moreover, TMB was calculated using Strawberry Perl in both LUAD and LUSC, and correlation of *IER5L* expression levels with TMB was evaluated using Spearman rank correlation analysis.

Construction of the Upstream Regulatory Network of *IER5L*

TFs were obtained from the Harmonizome (<https://maayanlab.cloud/Harmonizome/>) and GRNdb (<http://www.grndb.com/>) databases. miRNAs of *IER5L* were acquired from the miRWalk (<http://mirwalk.umm.uni-heidelberg.de/>), TargetScan (https://www.targetscan.org/vert_80/), and mirDIP (<http://ophid.utoronto.ca/mirDIP/>) databases.

Identification of Differentially Expressed Genes (DEGs) and Construction of a PPI Network

DEGs were identified between the two *IER5L* expression groups in NSCLC using the “limma” package in R language, and the criteria were $|\log_2$ fold change (FC) ≥ 1 and adjusted $P < 0.05$. A heatmap was generated between the two *IER5L* expression groups using the “pheatmap” package in R language. The STRING online database (<https://string-db.org>, version 11.0) was used to construct a PPI network.²² The top 200 DEGs were uploaded into the STRING online database to construct a PPI network, tailoring to “human”, “minimum required interaction score: 0.04”, and “network display options: hide disconnected nodes in the network”, and a “string_interactions_short.tsv” file was acquired. This file was then imported into Cytoscape (version 3.7.1) to identify hub genes using the MCC algorithm of cytoHubba app.

Functional Enrichment Analysis and GSEA

Functional enrichment analysis was performed using “clusterProfiler”, “org.Hs.eg.db”, “enrichplot” and “ggplot2” packages in R language, including biological process (BP), molecular function (MF), and cellular component (CC). Terms with adjusted $P < 0.05$ were considered of statistical significance. GSEA can determine whether a defined set of genes shows statistically significant and concordant differences between the two biological states.²³ GSEA software (version 4.0.3) and “c2.cp.kegg.v7.5.1.symbols.gmt” were obtained from the GSEA database (<http://www.gsea-msigdb.org/gsea/index.jsp>) and was used to perform pathway analysis between the two expression groups. Statistical significance was defined as false discovery rate (FDR) < 0.25 and adjusted $P < 0.05$.

Correlation of *IER5L* mRNA Expression with Immune Infiltration

Tumor micro-environment score was acquired using the “limma” and “e1071” packages in R language. The “vioplot” package in R language was used to calculate immune infiltration profiles between the two expression groups. In addition, correlations of *IER5L* expression with immune infiltration were assessed using Spearman rank correlation analysis in R language, and statistical significance was set at a P -value of < 0.05 and $|r| > 0.1$.

Correlation of *IER5L* mRNA Expression with Immune Molecules

Correlations of *IER5L* mRNA expression with multiple immune molecules (inhibitors and stimulators) in different cancers were obtained from the TISIDB database (<http://cis.hku.hk/TISIDB/index.php>). Correlations were assessed using Spearman rank correlation analysis.

Statistical Analysis

R language (version 4.0.2) and GraphPad Prism (version 7.00) were applied to perform statistical analysis and to draw all figures. Shapiro–Wilk normality test was used to evaluate data distribution type. Levels of *IER5L* relative expression were displayed as median (interquartile range). Comparisons between the two groups were performed using the Mann–Whitney test for nonparametric data. Kruskal–Wallis test was performed for multiple comparisons for nonparametric data. Correlation analysis was performed using Spearman rank correlation analysis. Survival curve was compared using Log rank test. Statistical significance was set at a P -value of < 0.05.

Results

IER5L Was Associated with Prognosis and Progression in a Pan-Cancer Analysis

We firstly performed a pan-cancer analysis of *IER5L* in GEPIA2 database. Levels of *IER5L* mRNA expression were increased in bladder urothelial carcinoma, breast invasive carcinoma (BRCA), cholangiocarcinoma, colon adenocarcinoma, esophageal carcinoma (ESCA), head and neck squamous cell carcinoma, LUAD, LUSC, rectum adenocarcinoma (READ), stomach adenocarcinoma, thyroid carcinoma (THCA), and uterine corpus endometrial carcinoma when compared with controls ($P < 0.05$, Figure 1A–C), while levels of *IER5L* mRNA expression were lower in kidney chromophobe (KICH) than corresponding controls ($P < 0.05$, Figure 1A). Kaplan–Meier survival curves showed that the high *IER5L* expression was correlated with a lower OS probability than the low *IER5L* expression in cervical and endocervical cancer (CESC) (Log-rank $P = 0.072$), kidney papillary cell carcinoma (KIRP) (Log-rank $P = 0.064$), brain lower grade glioma (Log-rank $P < 0.001$), liver hepatocellular carcinoma (LIHC) (Log-rank $P = 0.017$), NSCLC (Log-rank $P < 0.001$), ovarian serous cystadenocarcinoma (Log-rank $P = 0.068$), READ (Log-rank $P = 0.025$), and uveal melanoma (UVM) (Log-rank $P = 0.008$) (Figure 2A–H). Moreover, patients with the high *IER5L* expression displayed a worse DFS in comparison with patients with the low *IER5L* expression in BRCA (Log-rank $P = 0.037$), KIRP (Log-rank $P = 0.02$), NSCLC (Log-rank $P = 0.007$), pancreatic adenocarcinoma (Log-rank $P = 0.063$), prostate adenocarcinoma (Log-rank $P < 0.001$), READ (Log-rank $P = 0.047$), and UVM (Log-rank $P = 0.026$) (Figure 2I–O). Besides, levels of *IER5L* mRNA expression were associated with tumor progression in adrenocortical carcinoma ($P = 0.070$), CESC ($P = 0.021$), diffuse large B-cell lymphoma ($P = 0.018$), ESCA ($P = 0.042$), KICH ($P = 0.025$), LIHC ($P = 0.021$), testicular germ cell tumor ($P = 0.051$), THCA ($P = 0.002$), uterine carcinosarcoma ($P = 0.019$) (Figure 3A–I). Therefore, these findings show that *IER5L* expression is upregulated in multiple cancers and is associated with disease progression and prognosis.

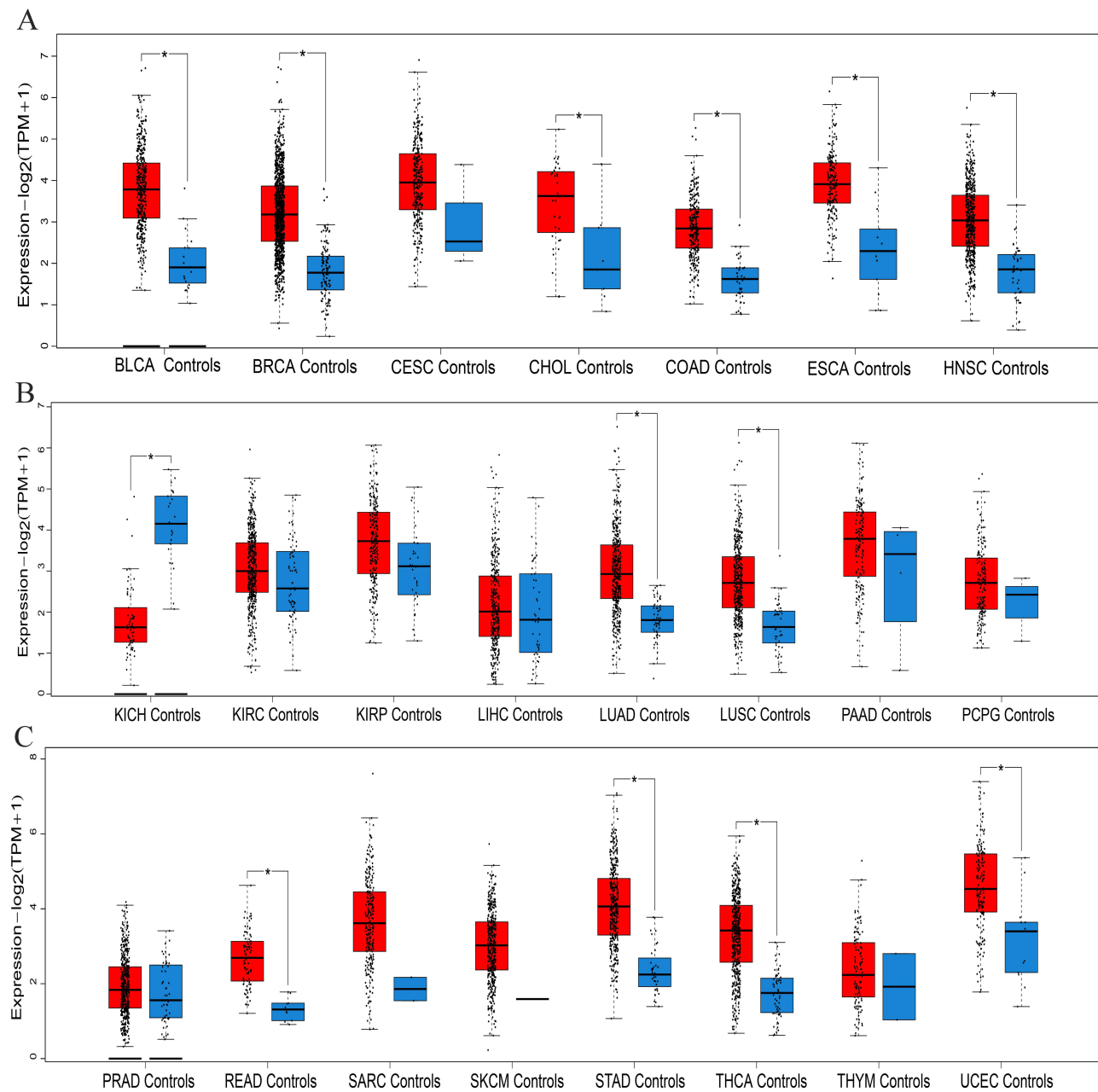


Figure 1 Levels of *IER5L* expression in 23 kinds of cancers and corresponding controls from GEPIA2 database. **(A)** BLCA, BRCA, CESC, CHOL, COAD, ESCA, NHSC. **(B)** KICH, KIRC, KIRP, LIHC, LUAD, LUSC, PAAD, PCPG. **(C)** PRAD, READ, SARC, SKCM, STAD, THCA, THYM, UCEC. * $P < 0.05$.

Abbreviations: *IER5L*, immediate early response 5 like; GEPIA2, Gene Expression Profiling Interactive Analysis 2.

IER5L as a Diagnostic Biomarker in NSCLC

Because of its increasing prevalence and mortality, NSCLC was selected as the focus of this study. Levels of *IER5L* mRNA expression were significantly higher in NSCLC tissues than in control tissues in the TCGA ($P < 0.001$, Figure 4A). The area under the curve (AUC) value was 0.882 (0.857–0.906), and cutoff value was 2.595 with a sensitivity of 74.25% and a specificity of 91.67% (Figure 4B). In addition, there were increased levels of *IER5L* expression in NSCLC in comparison with controls in both GSE31210 ($P = 0.005$; Figure 4C) and GSE30219 ($P < 0.001$; Figure 4D) datasets. qPCR was performed to validate the findings of bioinformatic analysis, and the results showed that levels of *IER5L* mRNA expression in NSCLC tissues were higher than those in control tissues ($P = 0.015$, Figure 4E).

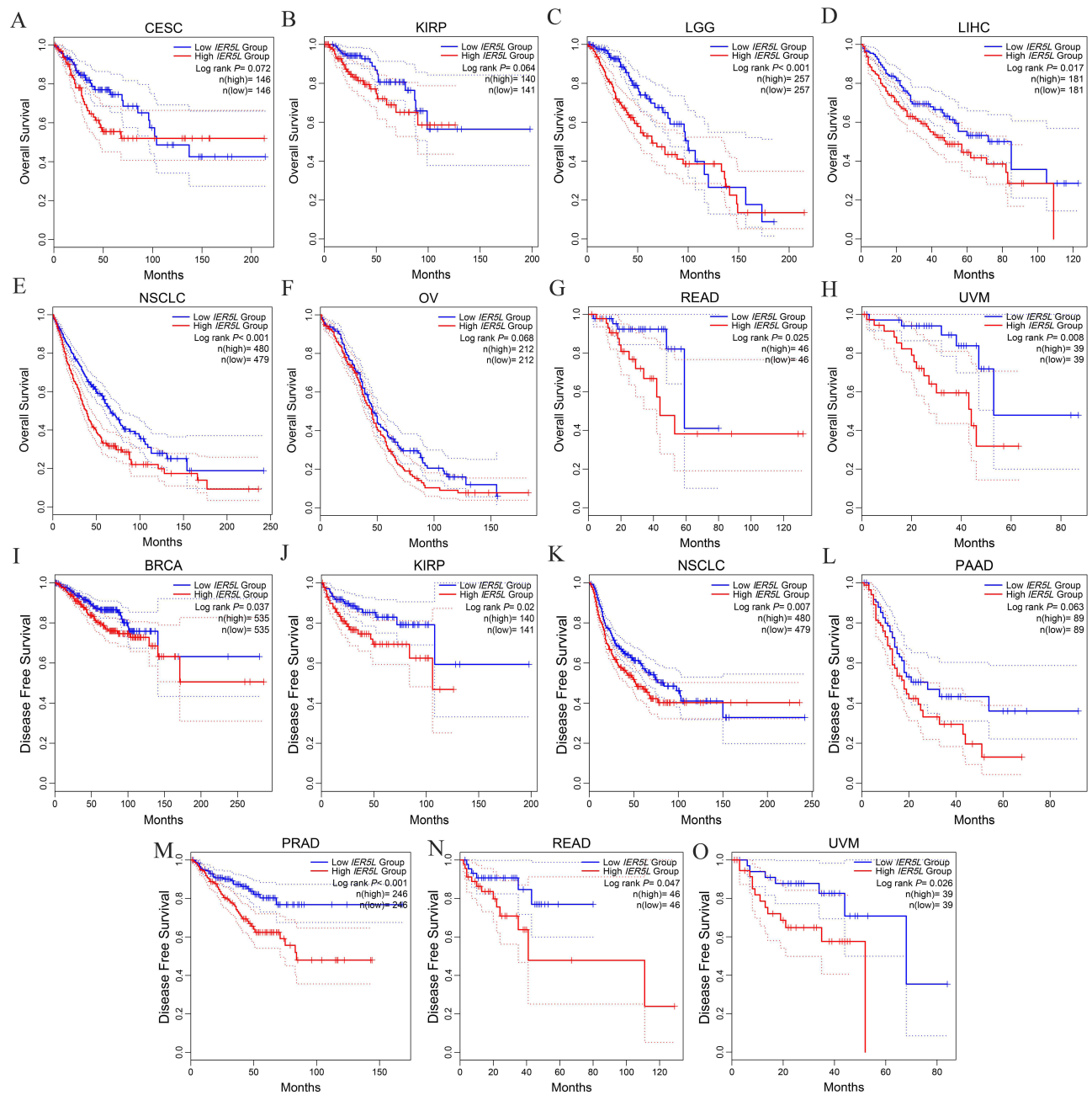


Figure 2 Kaplan-Meier survival analysis of *IER5L* in different tumors. (A-H) Overall survival between the two *IER5L* groups in CESC, KIRP, LGG, LIHC, NSCLC, OV, READ, and UVM. (I-O) Disease free survival between the two *IER5L* groups in BRCA, KIRP, NSCLC, PAAD, PRAD, READ, and UVM.

Abbreviation: *IER5L*, immediate early response 5 like.

Single-Cell RNA Sequencing Analysis

Single-cell RNA sequencing analysis was performed to explore source of overexpressed *IER5L* in NSCLC. A heatmap of six datasets is displayed in Figure 5A. *IER5L* was mainly expressed in malignant cells in NSCLC_GSE117570 (Figure 5A and B), in endothelial cells and fibroblasts in NSCLC_GSE127465 (Figure 5A and C), and in monocytes and macrophages in both NSCLC_GSE139555 (Figure 5A and D) and NSCLC_GSE99254 (Figure 5A and E).

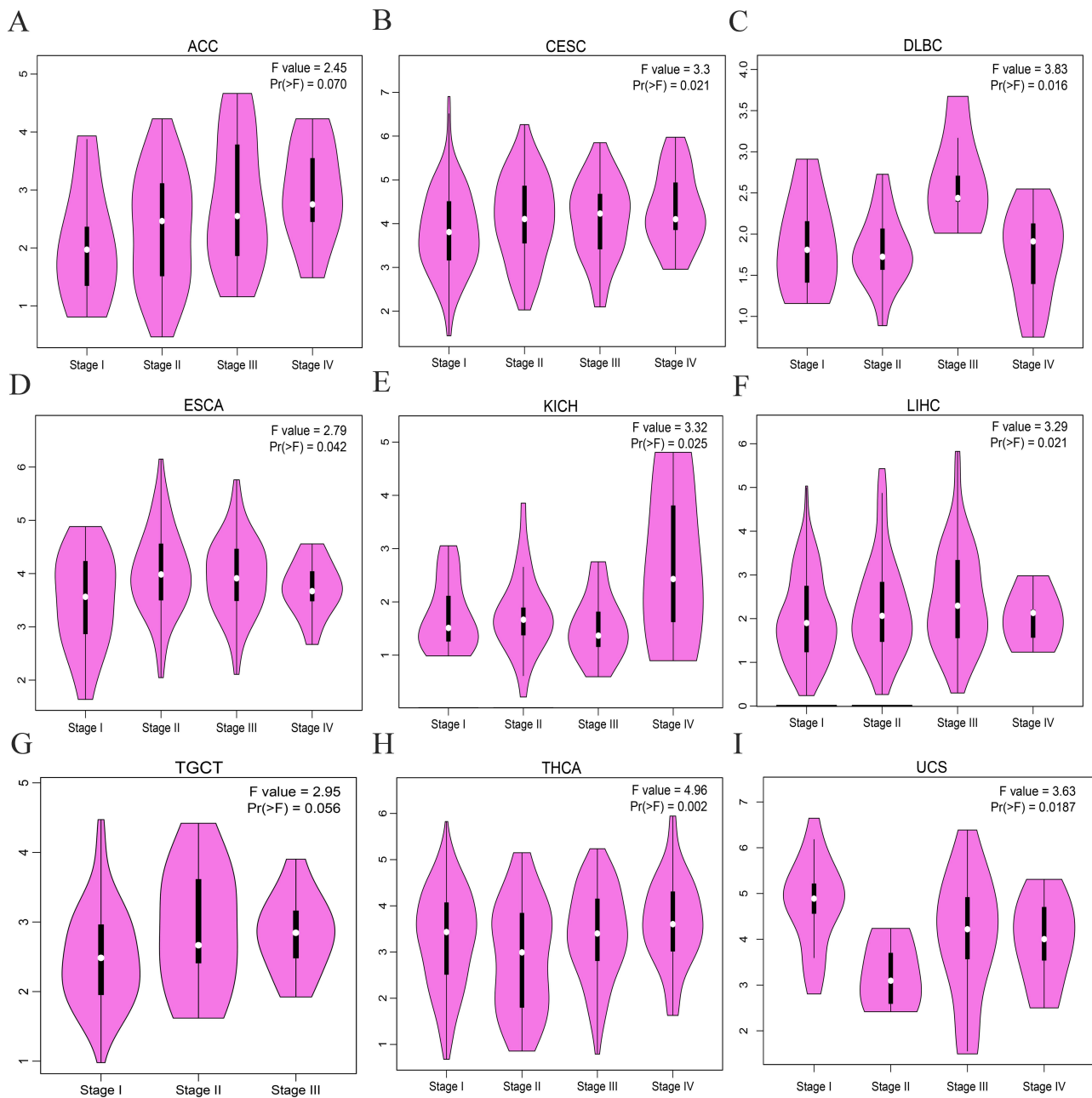


Figure 3 Correlation of *IER5L* expression with tumor stages. (A) ACC. (B) CESC. (C) DLBC. (D) ESCA. (E) KICH. (F) LIHC. (G) TGCT. (H) THCA. (I) UCS. *IER5L*, immediate early response 5 like.

IER5L Was a Prognostic Biomarker and Was Correlated with Clinical Characteristics in NSCLC

Kaplan–Meier survival curves showed that patients with the high *IER5L* mRNA expression had a lower OS probability than patients with the low *IER5L* mRNA expression in the TCGA ($P < 0.001$, Figure 6A), GSE31210 ($P < 0.001$, Figure 6B), and GSE30219 ($P < 0.001$, Figure 6C). In addition, the DFS probability was significantly lower in the high *IER5L* expression group than in the low *IER5L* expression group in GSE30219 ($P < 0.001$, Figure 6D). Levels of *IER5L* mRNA expression were higher in patients with stage III–IV cancer than in patients with stage I–II cancer in TCGA ($P = 0.001$, Figure 6E) and were increased in patients with stage II cancer than in patients with stage I cancer in GSE31210 ($P < 0.001$, Figure 6F). However, levels of *IER5L* mRNA expression were not a significant

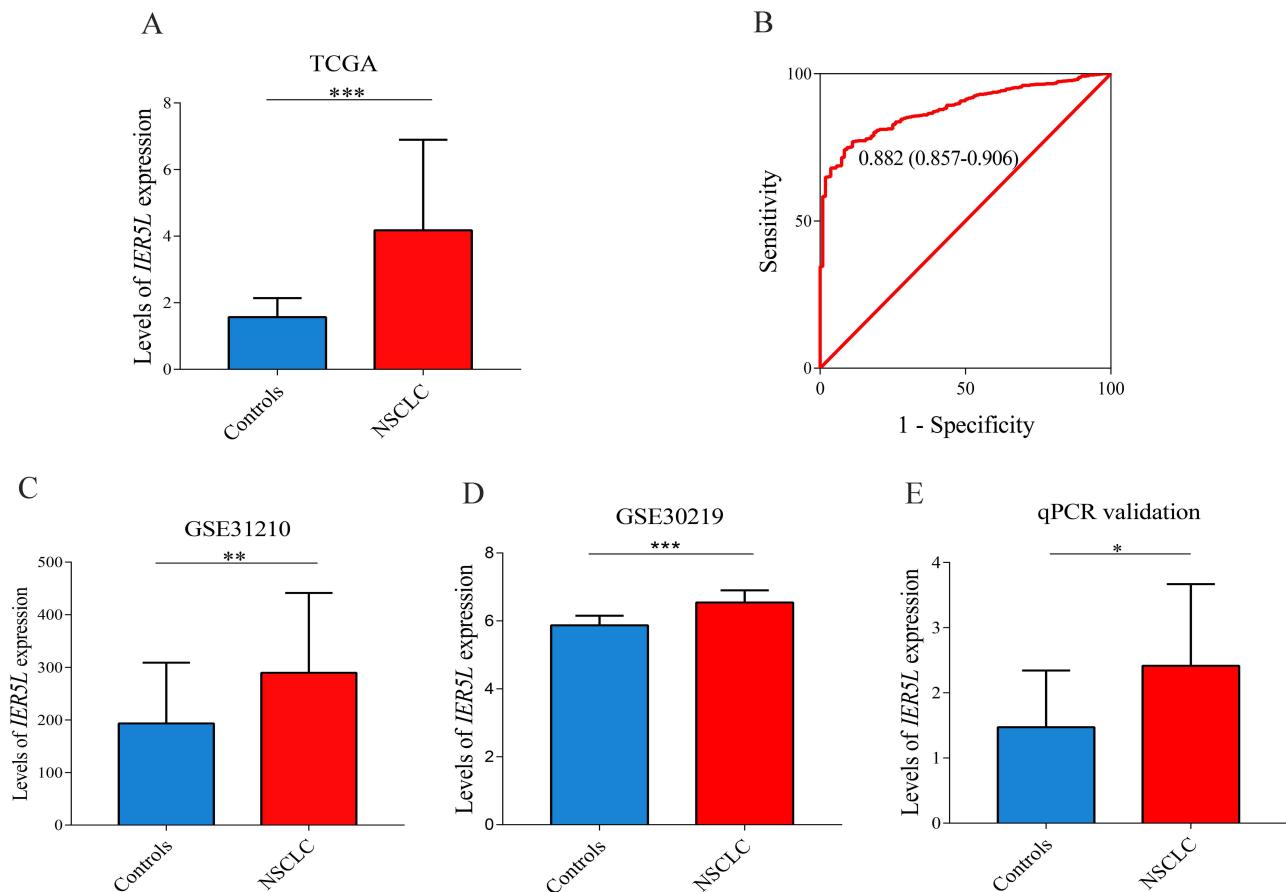


Figure 4 Levels of *IER5L* expression and its diagnostic value in NSCLC. **(A)** Levels of *IER5L* expression in NSCLC and corresponding controls from the TCGA. **(B)** Receiver operating characteristic curve of *IER5L* in NSCLC. **(C-E)** Levels of *IER5L* expression in NSCLC and corresponding controls from the GSE31210, GSE30219, and qPCR validation. *IER5L*, immediate early response 5 like; NSCLC, non-small cell lung cancer; TCGA, The Cancer Genome Atlas. * $P < 0.05$, ** $P < 0.01$, *** $P < 0.001$. **Abbreviation:** qPCR, quantitative polymerase chain reaction.

difference between stage I–II and stage III–IV in GSE30219 ($P > 0.05$, Figure 6G). The patients with relapse had higher levels of *IER5L* mRNA expression compared with the patients without relapse in GSE30219 ($P = 0.039$, Figure 6H).

IER5L as an Independent Prognostic Factor in NSCLC

Univariate Cox regression analysis reported that age (HR: 1.014; $P = 0.025$), UICC stage (HR: 1.475; $P < 0.001$), and *IER5L* expression (HR: 1.034; $P < 0.001$) were correlated with NSCLC prognosis (Figure 7A), which was confirmed using multivariate Cox regression analysis (for age, HR: 1.020, $P = 0.002$; for UICC stage, HR: 1.499; $P < 0.001$; for *IER5L* expression, HR: 1.037; $P < 0.001$, Figure 7B) in TCGA. In GSE30219, age (HR: 1.034; $P < 0.001$), T stage (HR: 1.568; $P < 0.001$), N stage (HR: 1.820; $P < 0.001$), and *IER5L* expression (HR: 1.536; $P = 0.003$) were correlated with prognosis using univariate Cox regression analysis (Figure 7C), and age (HR: 1.036; $P < 0.001$), N stage (HR: 1.646; $P < 0.001$), and *IER5L* expression (HR: 1.540; $P = 0.003$) were correlated with prognosis using multivariate Cox regression analysis (Figure 7D). In GSE31210, UICC stage (HR: 4.232; $P < 0.001$) and *IER5L* expression (HR: 1.001; $P = 0.035$) were correlated with NSCLC prognosis (Figure 7E), however, only UICC stage was correlated with prognosis using multivariate Cox regression analysis (HR: 3.928; $P < 0.001$, Figure 7F).

Nomogram and Calibration Plots of Nomogram

A nomogram was generated to predict OS probability, including age, UICC stage, and *IER5L* expression, in patients with NSCLC. The nomogram-predicted OS probability at 1, 3, and 5 years was calculated by plotting a vertical line between

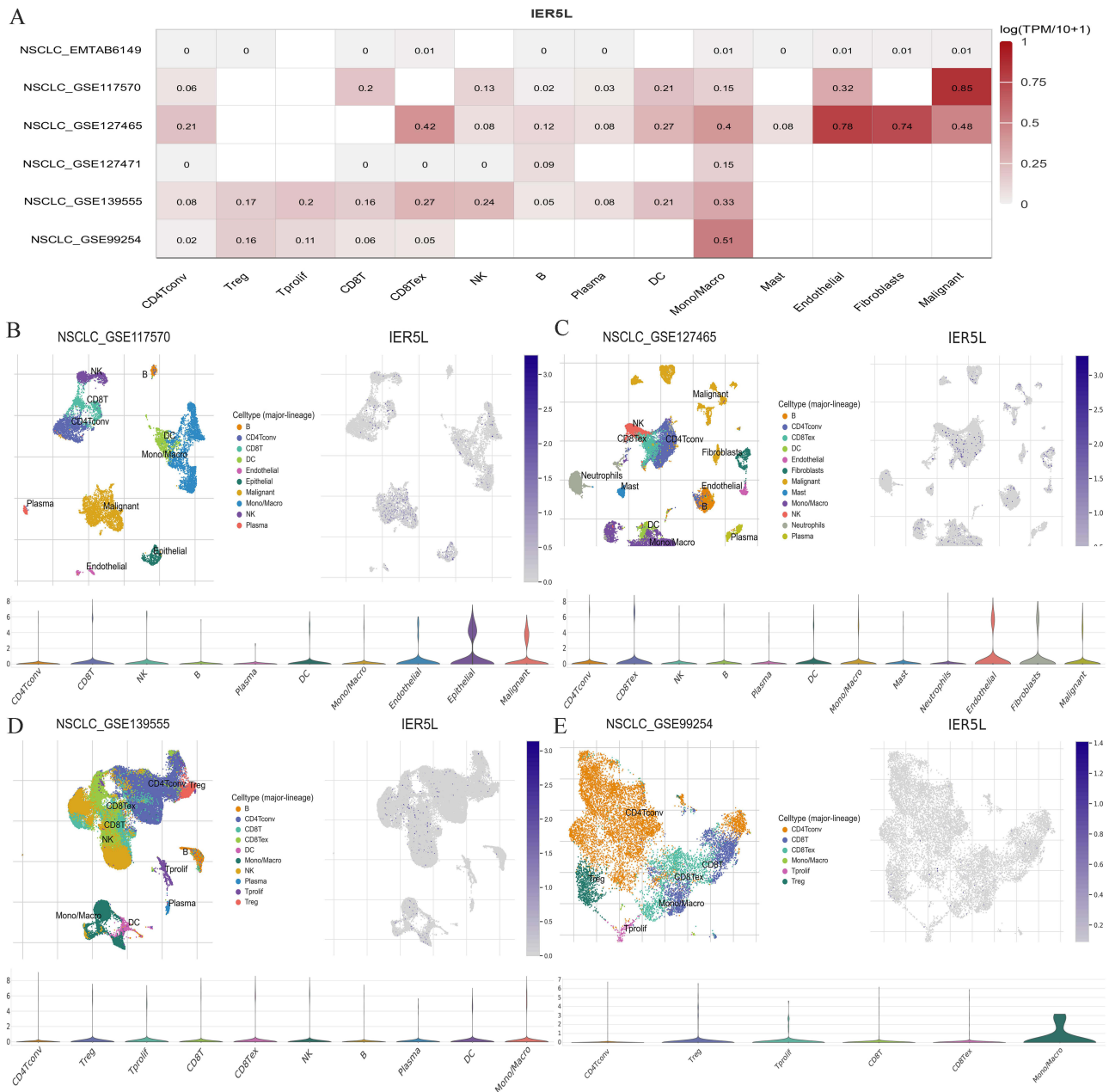


Figure 5 Single cell-RNA sequencing analysis in NSCLC. **(A)** A heatmap of six datasets. **(B-E)** Single-cell atlas and violin plot of *IER5L* in NSCLC_GSE117570, NSCLC_GSE127465, NSCLC_GSE139555, and NSCLC_GSE99254.

Abbreviations: NSCLC, non-small cell lung cancer; *IER5L*, immediate early response 5 like.

the total point axis and each prognostic axis (Figure 7G). Calibration plots of nomogram showed the high conformity of the nomogram-predicted and actual OS probability at 1, 3, and 5 years (Figure 7H).

IER5L Expression Was Correlated with TMB in NSCLC

Levels of *IER5L* methylation were negatively correlated with levels of *IER5L* mRNA expression without a statistical difference ($\rho = -0.05$, $P = 0.13$, Figure 8A). Genes with the highest mutation frequencies were tumor protein p53 (*TP53*) and titin (*TTN*) in both *IER5L* expression groups of LUAD and LUSC (Figure 8B-E). In addition, levels of *IER5L* mRNA expression were positively correlated with TMB in NSCLC ($\rho = 0.065$, $P = 0.043$, Figure 8F).

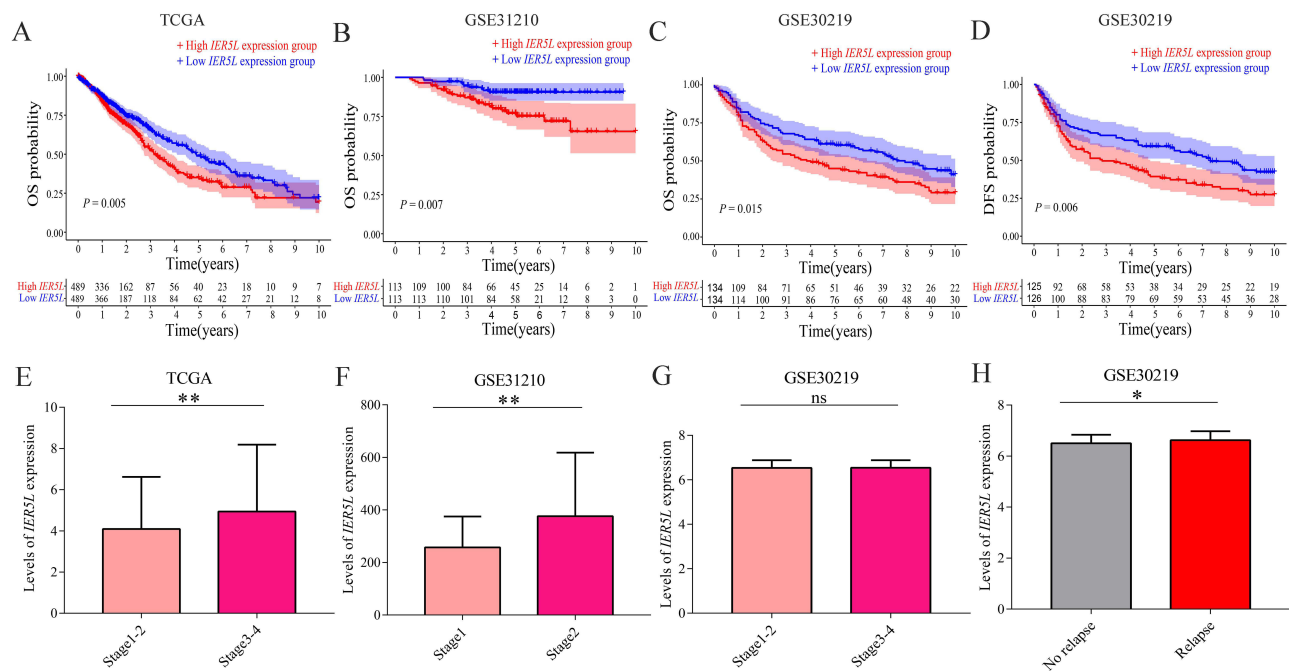


Figure 6 The clinical value of *IER5L* in NSCLC. (A-C) OS probability in the TCGA, GSE31210, and GSE30219. (D) DFS probability in the GSE30219. (E-G) Levels of *IER5L* expression in different UICC stages in TCGA, GSE31210, and GSE30219. (H) Levels of *IER5L* expression in different relapse groups in GSE30219. * $P < 0.05$, ** $P < 0.01$. **Abbreviations:** NSCLC, non-small cell lung cancer; *IER5L*, immediate early response 5 like; OS, overall survival; DFS, disease free survival; ns: no significance.

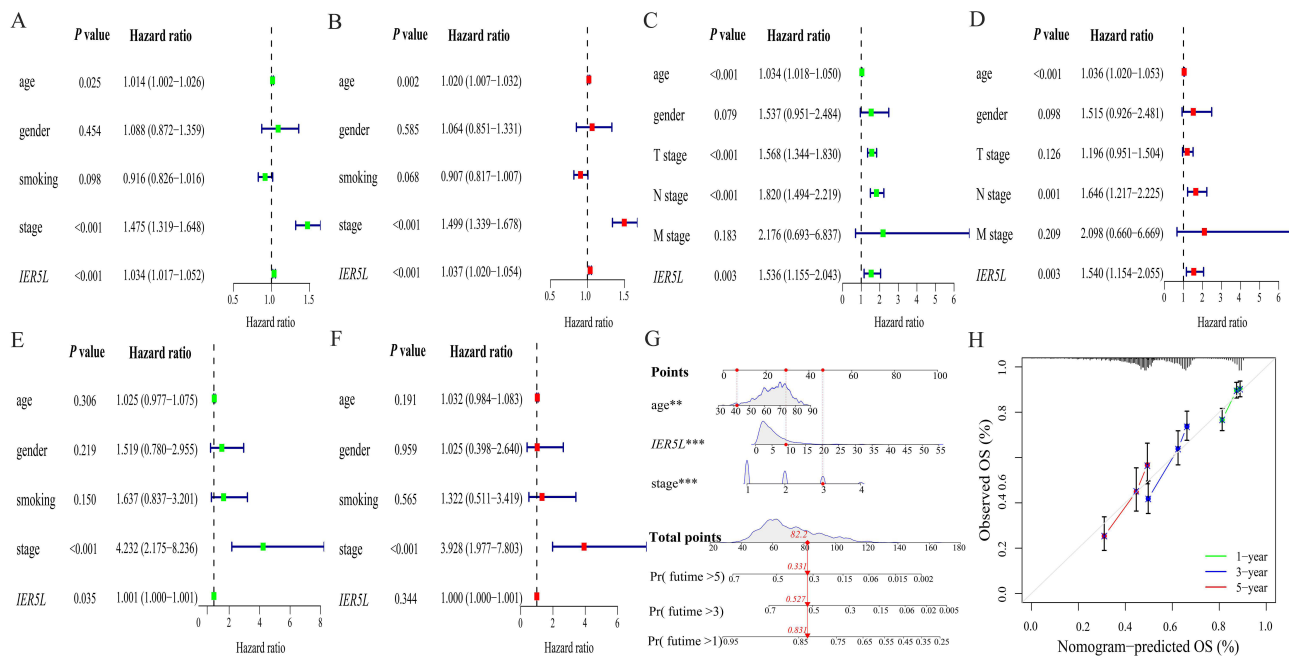
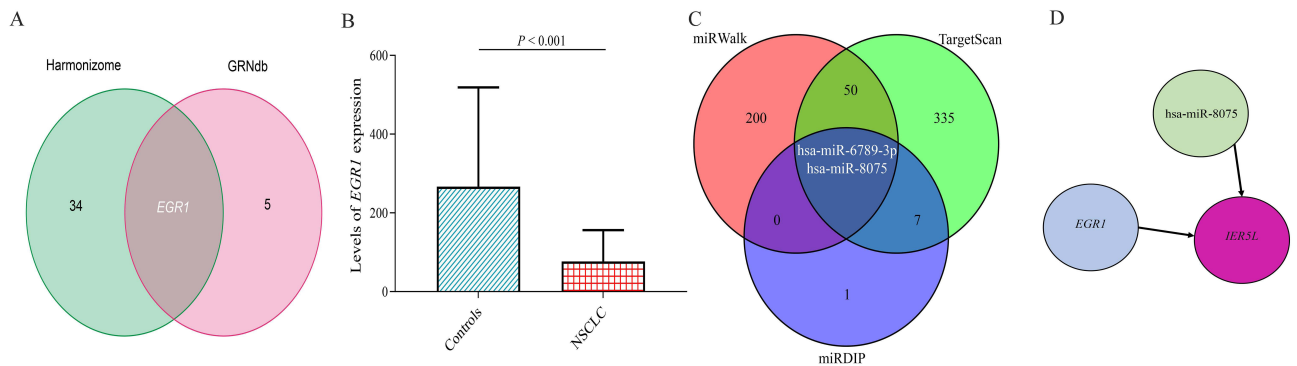
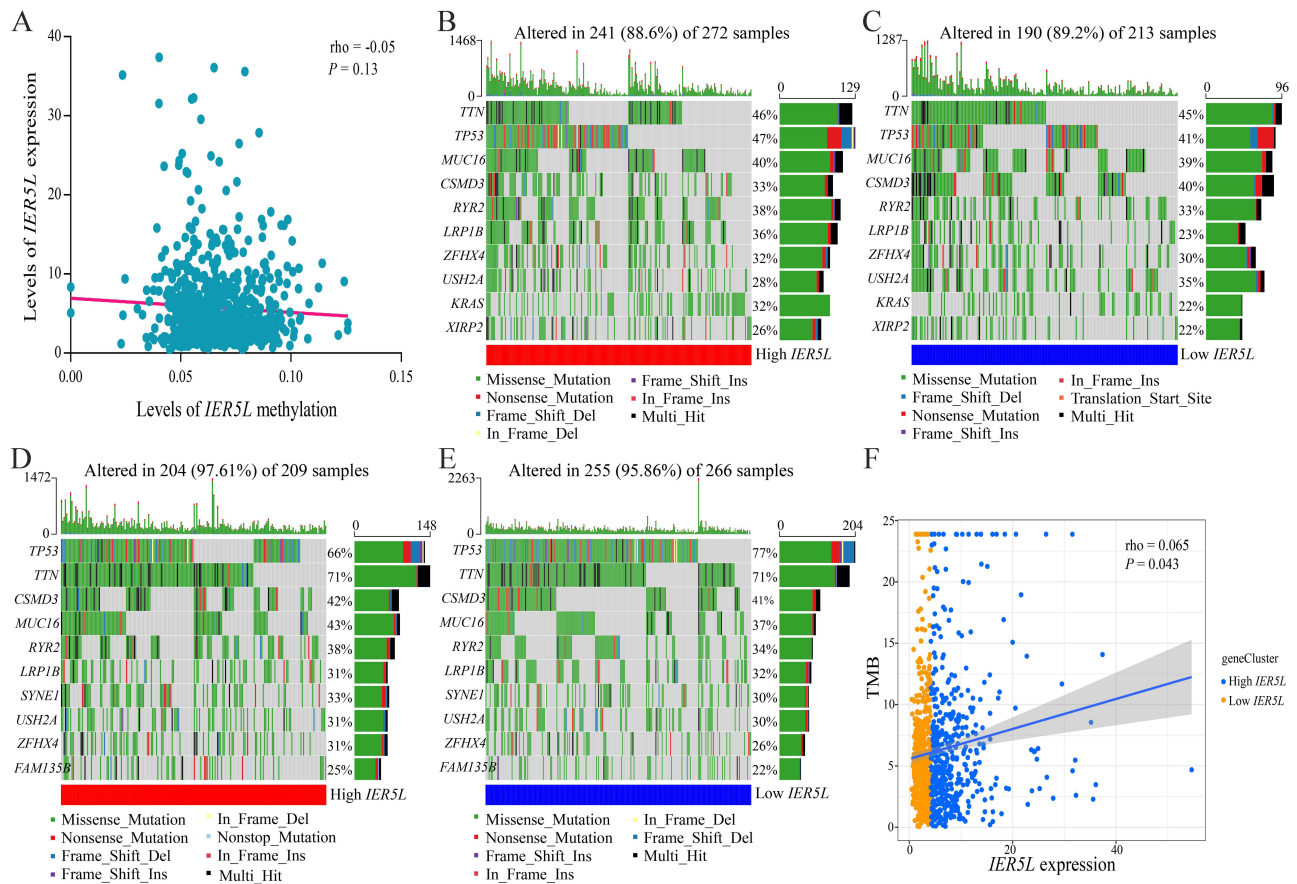


Figure 7 Univariate and multivariate Cox regression analysis, and a nomogram and its calibration plots. Univariate and multivariate Cox regression analyses in NSCLC in (A and B) TCGA, (C and D) GSE30219, and (E and F) GSE31210. (G) Nomogram. (H) Calibration plots of the nomogram. ** $P < 0.01$, *** $P < 0.001$. **Abbreviations:** *IER5L*, immediate early response 5 like; OS, overall survival.

An Upstream Regulatory Network of *IER5L* in NSCLC

There were 35 and 6 TFs from the Harmonizome and GRNdb databases, respectively, and early growth response 1 (*EGR1*) was the only overlapping TF between the two databases (Figure 9A). Levels of *EGR1* mRNA expression were decreased in NSCLC compared with controls ($P < 0.001$, Figure 9B). There were 252 miRNAs, 394 miRNAs, and 10



miRNAs from miRWalk, TargetScan, and miRDIP databases, respectively, and *hsa-miR-6789-3p* and *hsa-miR-8075* were overlapping miRNAs between the three databases (Figure 9C). *hsa-miR-8075* has been associated with tumor cell proliferation and invasion.^{24,25} Therefore, an *EGR1*-*hsa-miR-8075*-*IER5L* network was constructed in NSCLC (Figure 9D).

Identification of DEGs, Construction of a PPI Network, Functional Enrichment Analysis, and GSEA

A total of 191 DEGs (38 upregulated and 153 downregulated genes) were identified when comparing the high *IER5L* expression group with the low *IER5L* expression group ($|\log_2$ fold FC ≥ 1 and adjusted $P < 0.05$). A heatmap is illustrated in Figure 10A. A PPI network was generated in the STRING online database and the top 30 hub genes were screened using the MCC method in Cytoscape, among which the top five hub genes were neurotrophic receptor tyrosine kinase 2 (*NTRK2*), contactin 2 (*CNTN2*), synaptoporin (*SYNPR*), glutamate ionotropic receptor AMPA type subunit 1 (*GRI1A1*), and keratin 20 (*KRT20*) (Figure 10B). These DEGs were significantly enriched in BP such as action potential, sodium ion transport, and regulation of membrane potential; CC such as intermediate filament, intermediate filament cytoskeleton, and cation channel complex; and MF such as channel activity, passive transmembrane transporter activity, and mono-oxygenase activity (adjusted $P < 0.05$, Figure 10C). GSEA showed that pathways correlated with the high *IER5L* expression were primarily enriched in cell cycle, DNA replication, Notch signaling pathway, oxidative phosphorylation, base excision repair, and nucleotide excision repair (FDR <0.25 and nominal $P < 0.05$; Figure 10D-I).

IER5L Expression Was Correlated with Immune Infiltration

There was an increased number of regulatory T (Treg) cells ($P < 0.001$), neutrophils ($P < 0.05$), and activated natural killer (NK) cells ($P < 0.001$) in the high *IER5L* expression group in comparison with the low *IER5L* expression group (Figure 11A); whereas a reduced number of naive B cells ($P < 0.001$), resting memory CD4+ T cells ($P < 0.01$), resting dendritic cells ($P < 0.001$), resting mast cells ($P < 0.001$), and eosinophils ($P < 0.01$) in the high *IER5L* expression group compared with the low *IER5L* expression group (Figure 11A). Levels of *IER5L* expression were positively correlated with the number of Treg cells ($\rho = 0.19$, $P < 0.001$) and activated NK cells ($\rho = 0.14$, $P < 0.001$) (Figure 11B and C), and were negatively correlated with the number of naive B cells ($\rho = -0.13$, $P < 0.001$), resting memory CD4+ T cells ($\rho = -0.12$, $P < 0.001$), resting dendritic cells ($\rho = -0.17$, $P < 0.001$), and resting mast cells ($\rho = -0.17$, $P < 0.001$) (Figure 11D-G).

IER5L Expression Was Correlated with Immune Molecules

We next explored the correlation of *IER5L* with immune molecules including inhibitors and stimulators in the TISIDB database. *IER5L* mRNA expression was positively correlated with many immune inhibitors in NSCLC (Figure 12A). The top three immune inhibitors were nectin cell adhesion molecule 2 (*PVRL2*) ($\rho = 0.274$, $P < 0.001$), lymphocyte activating 3 (*LAG3*) ($\rho = 0.161$, $P < 0.001$), and programmed cell death 1 (*PDCD1*) ($\rho = 0.154$, $P < 0.001$) in LUAD (Figure 12B), and the top three immune inhibitors were transforming growth factor beta 1 (*TGFBI*) ($\rho = 0.337$, $P < 0.001$), *PVRL2* ($\rho = 0.336$, $P < 0.001$), and adenosine A2a receptor (*ADORA2A*) ($\rho = 0.082$, $P = 0.066$) in LUSC (Figure 12C). Besides, *IER5L* expression was positively correlated with many immune stimulators in NSCLC (Figure 12D). The top three immune stimulators were TNF receptor superfamily member 4 (*TNFRSF4*) ($\rho = 0.316$, $P < 0.001$), TNF receptor superfamily member 18 (*TNFRSF18*) ($\rho = 0.26$, $P < 0.001$), and CD276 molecule (*CD276*) ($\rho = 0.252$, $P < 0.001$) in LUAD (Figure 12E), and the top three immune stimulators were PVR cell adhesion molecule (*PVR*) ($\rho = 0.276$, $P < 0.001$), TNF receptor superfamily member 25 (*TNFRSF25*) ($\rho = 0.267$, $P < 0.001$), and retinoic acid early transcript 1E (*RAET1E*) ($\rho = 0.246$, $P < 0.001$) in LUSC (Figure 12F).

Discussions

In the current study, our findings showed that *IER5L* expression was dysregulated in multiple cancers and was also correlated with progression and prognosis in multiple cancers. In NSCLC, *IER5L* was a diagnostic biomarker and was an independent prognostic factor. An *EGR1*-hsa-miR-8075-*IER5L* network was constructed for NSCLC. DEGs are significantly enriched in the biological process of action potential, sodium ion transport, and regulation of membrane potential. Increased *IER5L* expression was primarily enriched in pathways of cell cycle, NOTCH signaling, and oxidative phosphorylation and was correlated with increased regulatory T cells and neutrophils, elevated levels of immune molecules, and high TMB.

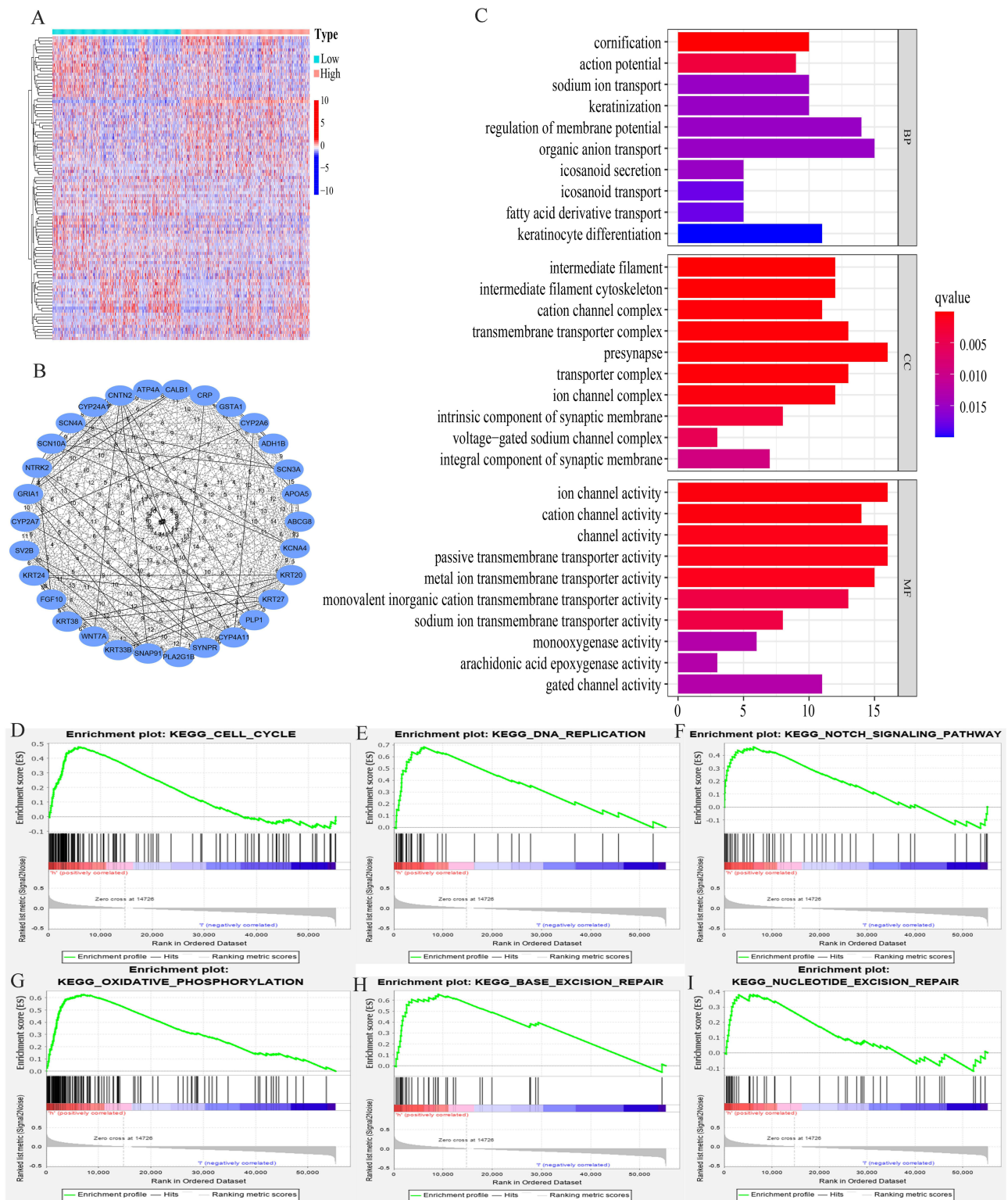


Figure 10 A PPI network, functional enrichment analysis, and gene set enrichment analysis. **(A)** A heatmap of two *IER5L* expression groups. **(B)** A PPI network. **(C)** Functional enrichment analysis, including BP, CC, and MF. **(D)** Cell cycle. **(E)** DNA replication. **(F)** Notch signaling pathway, **(G)** Oxidative phosphorylation. **(H)** Base excision repair. **(I)** Nucleotide excision repair.

Abbreviations: PPI, protein–protein interaction; BP, biological process; CC, cellular component; MF, molecular function; *IER5L*, immediate early response 5 like.

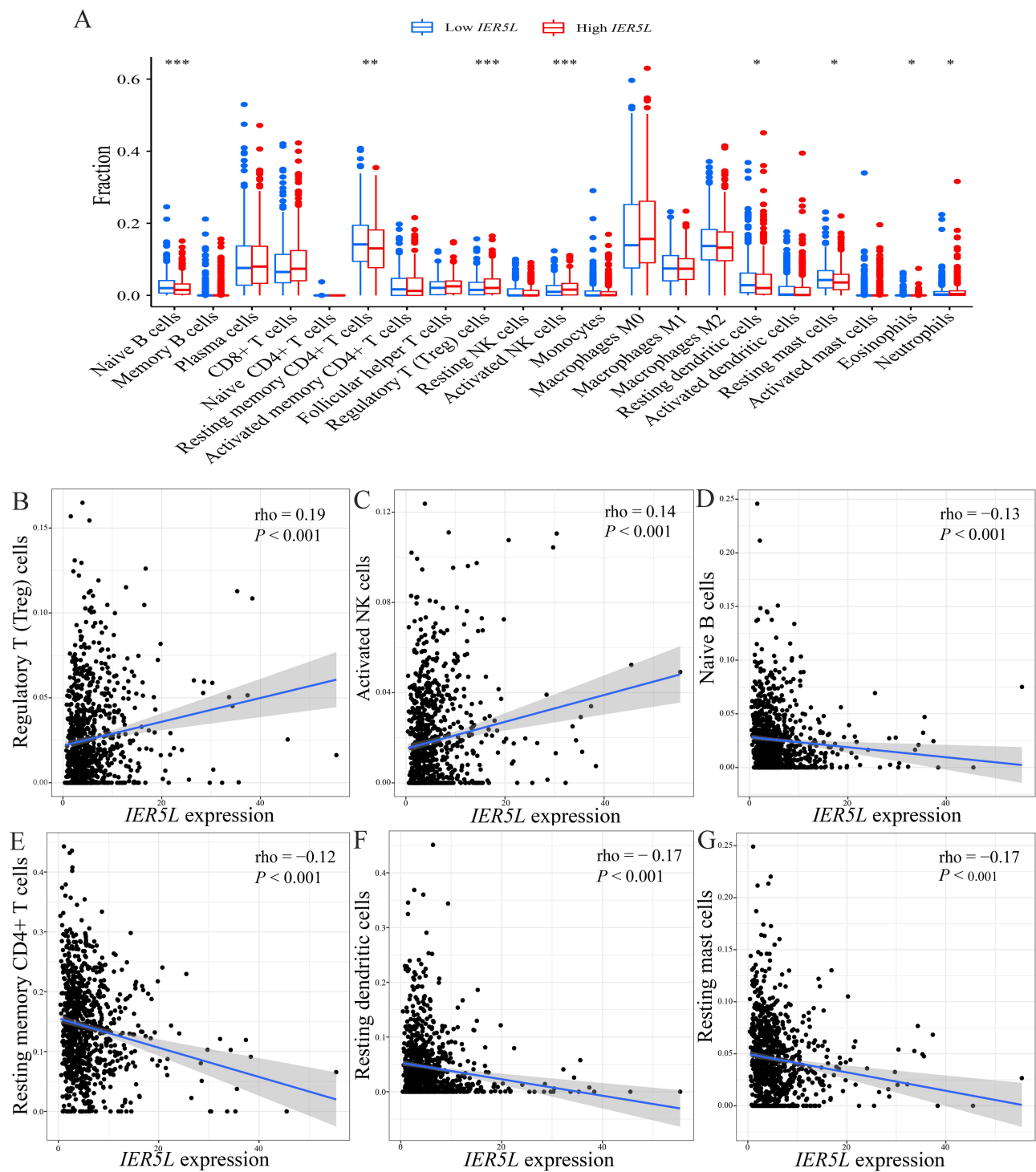


Figure 11 Correlations of *IER5L* expression with immune infiltration. **(A)** Immune infiltration profiles between the two *IER5L* expression groups. Correlations of *IER5L* expression with **(B)** Treg cells, **(C)** activated NK cells, **(D)** naive B cells, **(E)** resting memory CD4+ T cells, **(F)** resting dendritic cells, **(G)** resting mast cells. * $P < 0.05$, ** $P < 0.01$, *** $P < 0.001$.

Abbreviations: *IER5L*, immediate early response 5 like; Treg, regulatory T; NK, natural killer.

Previous studies have shown that levels of *IER5L* expression were increased in both primary tumor tissues and metastatic tumor tissues and were negatively correlated with survival.^{20,21} Our study showed that *IER5L* expression was upregulated in many kinds of tumors in various systems and was associated with UICC stages and prognosis. Thus, in combination with the previous findings, we could conclude that *IER5L* may be a diagnostic and prognostic biomarker in

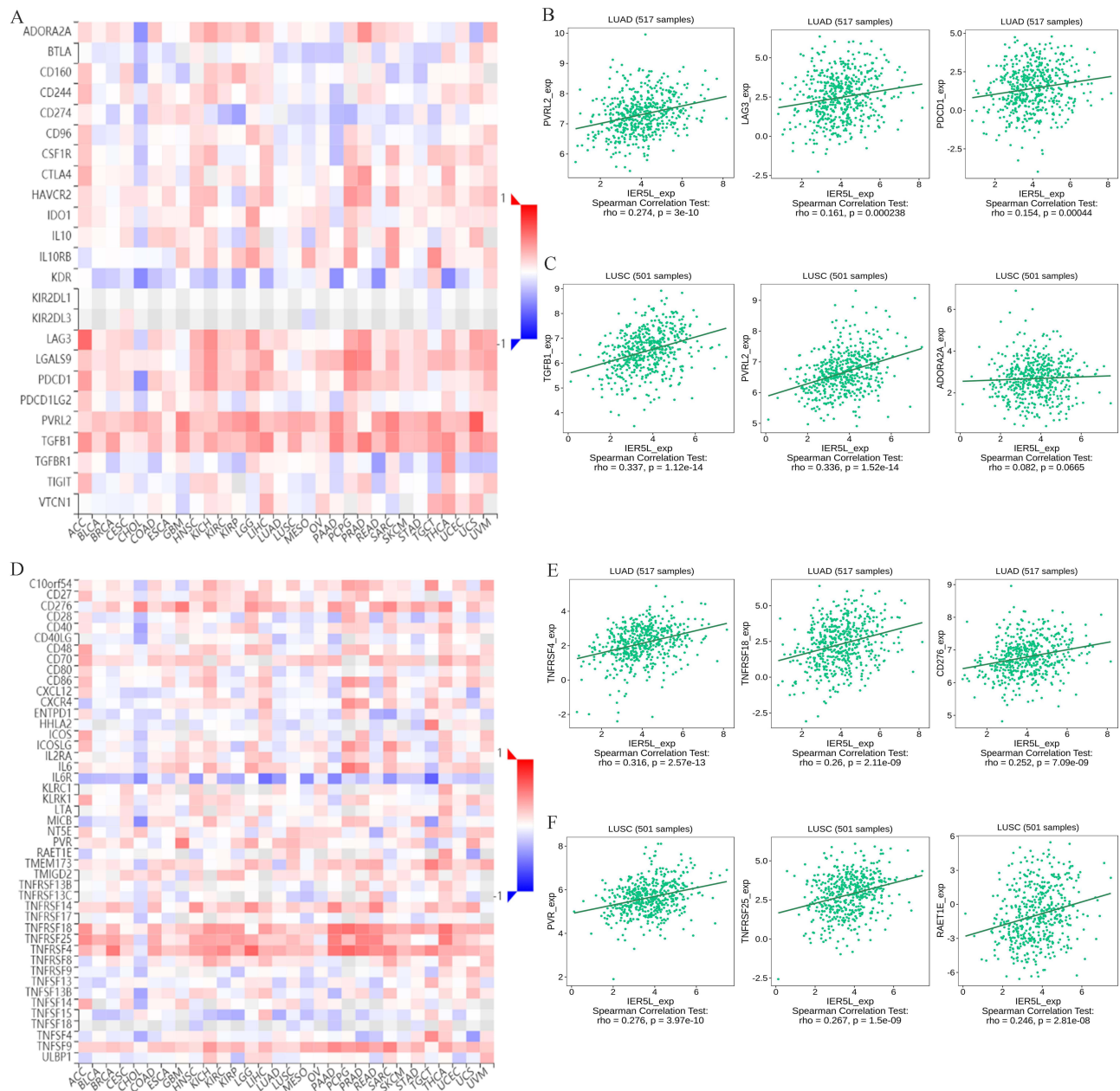


Figure 12 Correlations of *IER5L* expression with immune molecules. **(A)** Correlations of *IER5L* expression with immune inhibitors in multiple cancers. **(B and C)** The top 3 immune inhibitors in lung adenocarcinoma and lung squamous cell carcinoma. **(D)** Correlations of *IER5L* expression with immune stimulators in multiple cancers. **(E and F)** The top 3 immune stimulators in lung adenocarcinoma and lung squamous cell carcinoma.

Abbreviation: *IER5L*, immediate early response 5 like.

cancer. Similar results have also been confirmed in NSCLC using several datasets, and increased *IER5L* expression has been validated using qPCR. In addition, univariate and multivariate Cox regression analyses reported that *IER5L* expression was correlated with NSCLC prognosis after adjustment for age and UICC stage. Thus, *IER5L* is an independent prognostic factor for NSCLC. A nomogram was generated using independent prognostic factors, and calibration plots of the nomogram showed highly predictive accuracy.

We then explore the underlying downstream mechanisms between the two *IER5L* expression groups using GSEA. The oxidative phosphorylation, Notch signaling pathway, cell cycle, and DNA replication were the primary pathways in our study. Increasing evidences reveal that oxidative phosphorylation is more active in cancer cells than in normal cells,²⁶ Attenuating cell oxidative phosphorylation could suppress cancer cell migration and invasion.^{27,28} The Notch signaling

pathway has been implicated in the pathogenesis of many cancers,^{29–31} and it influences tumor microenvironment,³² and predicts prognosis, recurrence, and response to therapy.^{33–36} Deregulation in cell cycle progression result in the unconstrained tumor cell proliferation.³⁷ DNA replication must be precisely controlled to maintain genome stability,³⁸ and genome instability increases the risk of cancer.³⁹ Thus, *IER5L* may be involved in the tumorigenesis, progression, and prognosis of NSCLC through the above-mentioned pathways. However, these pathways may not function as an isolated state; instead, they may interact to influence roles of tumor cells. Thus, more researches were needed to explore potential mechanisms between these pathways and role of *IER5L* in these pathways. TMB has been associated with prognosis of disease and immunotherapeutic response in multiple cancers.⁴⁰ Our study has reported that increased *IER5L* expression was correlated with higher TMB. Thus, the worse prognosis in the high *IER5L* expression may be correlated with increased TMB. These results show that interfering *IER5L* may prevent progression and improve prognosis in NSCLC, and it deserves further investigation.

The tumor microenvironment is mainly composed of malignant cells, fibroblasts, immune cells, and endothelial cells,⁴¹ and they play critical roles in initiation, progression, and prognosis in cancer.⁴² Treg cells are abundant in NSCLC and have an increased risk of recurrence in early-stage cancer,⁴³ and could predict the efficacy of *PD-1/PD-L1* inhibitors.⁴⁴ Additionally, increased tumor-infiltrating Treg cells are associated with lower OS and DFS probability in lung cancer.^{45–47} Lung cancer tissues have more neutrophil infiltration and neutrophil extracellular traps (NETs) formation.⁴⁸ Neutrophils are higher in advanced NSCLC⁴⁹ and are independently associated with survival.⁵⁰ Moreover, NETs can enable A549 cells to invade and migrate in a macrophage-maintained inflammatory microenvironment.⁴⁸ Brain metastasis of lung cancer is correlated with nicotine-induced N2-neutrophils.⁵¹ Resting mast cells and eosinophils are significantly lower in lung cancer tissues.⁵² The increased Treg cells and neutrophils as well as reduced resting mast cells and eosinophils were reported in the high *IER5L* expression group in the current study. Thus, *IER5L* was correlated with a dysregulated immune microenvironment, and may be correlated with response on immunotherapy. Our results also showed that *IER5L* expression was positively correlated with many immune molecules. Increased *PDI* levels were significantly associated with better response to immunotherapy and worse OS probability,^{53,54} and *PDI/PDL1* complex had a higher predictive value compared with single *PDI*.⁵⁵ QL1706, a mixture of anti-*PDI* and anti-*CTLA4*, showed promising anti-tumor activities for immunotherapy-naive patients.⁵⁶ Thus, *IER5L* may function as an immunotherapeutic biomarker for NSCLC.

There are some highlights in our study. First, we have reported increased *IER5L* mRNA expression in multiple cancers, including NSCLC using multiple databases. Second, we performed comprehensive and in-depth bioinformatic analyses to explore the prognostic and therapeutic values of *IER5L* in NSCLC. Finally, qPCR validated the increased levels of *IER5L* mRNA expression in NSCLC. However, some limitations cannot be ignored in the current study. The current study is mainly based on bioinformatics analysis, and more experiments need to be performed to validate the function of *IER5L* in NSCLC. Moreover, the specific role of *IER5L* in cancer cell proliferation, migration, and invasion was not investigated in this study.

Conclusions

Pan-cancer analysis displayed that levels of *IER5L* expression were upregulated in multiple cancers and were associated with disease prognosis and progression, including NSCLC. An *EGR1*-hsa-miR-8075-*IER5L* network was constructed for NSCLC. DEGs are significantly enriched in the biological process of action potential, sodium ion transport, and regulation of membrane potential. Increased *IER5L* expression was primarily enriched in pathways of cell cycle, NOTCH signaling, and oxidative phosphorylation and was correlated with increased regulatory T cells and neutrophils, elevated levels of immune molecules, and high TMB. Thus, *IER5L* is a prognostic biomarker in multiple cancers and may correlate with immunotherapeutic response in NSCLC.

Abbreviations

ADAMDECI, ADAM-like decysin-1; AUC, area under the curve; BP, biological process; CC, cellular component; *CTLA4*, cytotoxic T-lymphocyte associated protein 4; DEGs, differentially expressed genes; DFS, disease-free survival; *ERBB4*, Erb-b2 receptor tyrosine kinase 4; FDR, False discovery rate; FC, fold change, GEO, Gene Expression Omnibus; GEPIA2, Gene Expression Profiling Interactive Analysis 2; GSEA, gene set enrichment analysis; *IER5L*, immediate early response 5 like;

NK, natural killer; *KAT2B*, lysine acetyltransferase 2B; MF, molecular function; NSCLC, non-small cell lung cancer; OS, overall survival; *PDI*, programmed cell death 1; *PDL1*, programmed cell death 1 ligand 1; PP1, protein–protein interaction, qPCR, quantitative polymerase chain reaction; ROC, receiver operating characteristic; *Siglec15*, sialic acid binding Ig-like lectin 15; scRNA seq, single-cell RNA sequencing; TCGA, The Cancer Genome Atlas; TMB, tumor mutation burden; UICC, Union for International Cancer Control; BRCA, breast invasive carcinoma, ESCA, esophageal carcinoma; READ, rectum adenocarcinoma; THCA, thyroid carcinoma; KICH, kidney chromophobe; CESC, cervical and endocervical cancer; KIRP, kidney papillary cell carcinoma; LIHC, liver hepatocellular carcinoma; UVM, uveal melanoma.

Data Sharing Statement

The datasets used and/or analyzed during the current study are available from the corresponding author on reasonable request.

Ethics Approval and Informed Consent

This study was approved by the Clinical Trial and Biomedical Ethics Committee of Zigong First People's Hospital (No.2021-24) and was conducted in accordance with the principles of Declaration of Helsinki. All patients volunteered to attend the study and signed an informed consent.

Author Contributions

All authors made a significant contribution to the work reported, whether that is in the conception, study design, execution, acquisition of data, analysis and interpretation, or in all these areas; took part in drafting, revising, or critically reviewing the article; gave final approval of the version to be published; have agreed on the journal to which the article has been submitted; and agree to be accountable for all aspects of the work.

Funding

This work was supported by Sichuan Provincial Administration of Traditional Chinese Medicine [2021MS462] and Key R&D Program of Zigong Science and Technology Bureau [2021YXY01].

Disclosure

The authors declare that they have no competing interests in this work.

References

1. Sung H, Ferlay J, Siegel RL, et al. Global Cancer Statistics 2020: GLOBOCAN Estimates of Incidence and Mortality Worldwide for 36 Cancers in 185 Countries. *CA Cancer J Clin.* 2021;71(3):209–249. doi:10.3322/caac.21660
2. Travis WD, Brambilla E, Burke AP, et al. Introduction to The 2015 World Health Organization Classification of Tumors of the Lung, Pleura, Thymus, and Heart. *J Thorac Oncol.* 2015;10(9):1240–1242. doi:10.1097/jto.0000000000000663
3. Molina JR, Yang P, Cassivi SD, et al. Non-small cell lung cancer: epidemiology, risk factors, treatment, and survivorship. *Mayo Clin Proc.* 2008;83(5):584–594. doi:10.4065/83.5.584
4. Bray F, Ferlay J, Soerjomataram I, et al. Global cancer statistics 2018: GLOBOCAN estimates of incidence and mortality worldwide for 36 cancers in 185 countries. *CA Cancer J Clin.* 2018;68(6):394–424. doi:10.3322/caac.21492
5. Allemani C, Matsuda T, Di Carlo V, et al. Global surveillance of trends in cancer survival 2000–14 (Concord-3): analysis of individual records for 37 513 025 patients diagnosed with one of 18 cancers from 322 population-based registries in 71 countries. *Lancet.* 2018;391(10125):1023–1075. doi:10.1016/s0140-6736(17)33326-3
6. Stella GM, Luisetti M, Pozzi E, et al. Oncogenes in non-small-cell lung cancer: emerging connections and novel therapeutic dynamics. *Lancet Respir Med.* 2013;1:251–261. doi:10.1016/s2213-2600(13)70009-2
7. Herbst RS, Morgensztern D, Boshoff C. The biology and management of non-small cell lung cancer. *Nature.* 2018;553(7689):446–454. doi:10.1038/nature25183
8. Zhu W, Shi L, Gong Y, et al. Upregulation of ADAMDEC1 correlates with tumor progression and predicts poor prognosis in non-small cell lung cancer (NSCLC) via the PI3K/AKT pathway. *Thorac Cancer.* 2022;13:1027–1039. doi:10.1111/1759-7714.14354
9. Zhang C, Huang J, Lou K, et al. Long noncoding RNASEH1-AS1 exacerbates the progression of non-small cell lung cancer by acting as a ceRNA to regulate microRNA-516a-5p/FOXK1 and thereby activating the Wnt/ β -catenin signaling pathway. *Cancer Med.* 2022;11:1589–1604. doi:10.1002/cam4.4509
10. Liang H, Chen Q, Hu Z, et al. Siglec15 facilitates the progression of non-small cell lung cancer and is correlated with spinal metastasis. *Ann Transl Med.* 2022;10(6):281. doi:10.21037/atm-22-764

11. Zhou X, Wang N, Zhang Y, et al. KAT2B is an immune infiltration-associated biomarker predicting prognosis and response to immunotherapy in non-small cell lung cancer. *Invest New Drugs*. 2022;40(1):43–57. doi:10.1007/s10637-021-01159-6
12. Hu X, Xu H, Xue Q, et al. The role of ERBB4 mutations in the prognosis of advanced non-small cell lung cancer treated with immune checkpoint inhibitors. *Mol Med*. 2021;27(1):126. doi:10.1186/s10020-021-00387-z
13. Miao TW, Chen FY, Du LY, et al. Signature based on RNA-binding protein-related genes for predicting prognosis and guiding therapy in non-small cell lung cancer. *Front Genet*. 2022;13:930826. doi:10.3389/fgene.2022.930826
14. Liu XG, Li M, Mai SJ, et al. Telomere length-related signature as a novel biomarker of prognosis and immune response in non-small cell lung cancer. *Eur Rev Med Pharmacol Sci*. 2022;26(4):1304–1319. doi:10.26355/eurrev_202202_28124
15. Li M, Zhang Y, Fan M, et al. Identification of the ferroptosis-related long non-coding RNAs signature to improve the prognosis prediction and immunotherapy response in patients with NSCLC. *BMC Med Genomics*. 2021;14(1):286. doi:10.1186/s12920-021-01133-4
16. Wang Q, Zhou D, Wu F, et al. Immune Microenvironment Signatures as Biomarkers to Predict Early Recurrence of Stage Ia-b Lung Cancer. *Front Oncol*. 2021;11:680287. doi:10.3389/fonc.2021.680287
17. Fang C, Liu F, Wang Y, et al. A innovative prognostic symbol based on neutrophil extracellular traps (NETs)-related lncRNA signature in non-small-cell lung cancer. *Aging*. 2021;13(13):17864–17879. doi:10.18632/aging.203289
18. Yao J, Li R, Liu X, et al. Prognostic implication of glycolysis related gene signature in non-small cell lung cancer. *J Cancer*. 2021;12(3):885–898. doi:10.7150/jca.50274
19. Ueda T, Kohama Y, Sakurai H. IER family proteins are regulators of protein phosphatase PP2A and modulate the phosphorylation status of CDC25A. *Cell Signal*. 2019;55:81–89. doi:10.1016/j.cellsig.2018.12.012
20. Vastrad C, Vastrad B. Bioinformatics analysis of gene expression profiles to diagnose crucial and novel genes in glioblastoma multiform. *Pathol Res Pract*. 2018;214(9):1395–1461. doi:10.1016/j.prp.2018.07.015
21. Zou J, Zhang H, Huang Y, et al. Multi-Omics Analysis of the Tumor Microenvironment in Liver Metastasis of Colorectal Cancer Identified FJX1 as a Novel Biomarker. *Front Genet*. 2022;13:960954. doi:10.3389/fgene.2022.960954
22. Szklarczyk D, Gable AL, Lyon D, et al. STRING v11: protein-protein association networks with increased coverage, supporting functional discovery in genome-wide experimental datasets. *Nucleic Acids Res*. 2019;47:D607–d613. doi:10.1093/nar/gky1131
23. Subramanian A, Tamayo P, Mootha VK, et al. Gene set enrichment analysis: a knowledge-based approach for interpreting genome-wide expression profiles. *Proc Natl Acad Sci U S A*. 2005;102(43):15545–15550. doi:10.1073/pnas.0506580102
24. Song T, Xu A, Zhang Z, et al. CircRNA hsa_circRNA_101996 increases cervical cancer proliferation and invasion through activating TPX2 expression by restraining miR-8075. *J Cell Physiol*. 2019;234(8):14296–14305. doi:10.1002/jcp.28128
25. Yan S, Han B, Gao S, et al. Exosome-encapsulated microRNAs as circulating biomarkers for colorectal cancer. *Oncotarget*. 2017;8(36):60149–60158. doi:10.18632/oncotarget.18557
26. Zacksenhaus E, Shrestha M, Liu JC, et al. Mitochondrial OXPHOS Induced by RB1 Deficiency in Breast Cancer: implications for Anabolic Metabolism, Stemness, and Metastasis. *Trends Cancer*. 2017;3(11):768–779. doi:10.1016/j.trecan.2017.09.002
27. Nie W, Hu MJ, Zhang Q, et al. DUBR suppresses migration and invasion of human lung adenocarcinoma cells via ZBTB11-mediated inhibition of oxidative phosphorylation. *Acta Pharmacol Sin*. 2022;43:157–166. doi:10.1038/s41401-021-00624-5
28. Zhang J, Yan L, Wei P, et al. PEG-GO@XN nanocomposite suppresses breast cancer metastasis via inhibition of mitochondrial oxidative phosphorylation and blockade of epithelial-to-mesenchymal transition. *Eur J Pharmacol*. 2021;895:173866. doi:10.1016/j.ejphar.2021.173866
29. Allen TD, Rodriguez EM, Jones KD, et al. Activated Notch1 induces lung adenomas in mice and cooperates with Myc in the generation of lung adenocarcinoma. *Cancer Res*. 2011;71(18):6010–6018. doi:10.1158/0008-5472.can-11-0595
30. Aster JC, Pear WS, Blacklow SC. The Varied Roles of Notch in Cancer. *Annu Rev Pathol*. 2017;12(1):245–275. doi:10.1146/annurev-pathol-052016-100127
31. Sharif A, Shaji A, Chamma M, et al. Notch Transduction in Non-Small Cell Lung Cancer. *Int J Mol Sci*. 2020;22(1):21. doi:10.3390/ijms21165691
32. Li X, Wang Y, Li X, et al. The Impact of NOTCH Pathway Alteration on Tumor Microenvironment and Clinical Survival of Immune Checkpoint Inhibitors in NSCLC. *Front Immunol*. 2021;12:638763. doi:10.3389/fimmu.2021.638763
33. Chen CY, Chen YY, Hsieh MS, et al. Expression of Notch Gene and Its Impact on Survival of Patients with Resectable Non-small Cell Lung Cancer. *J Cancer*. 2017;8(7):1292–1300. doi:10.7150/jca.17741
34. Donnem T, Andersen S, Al-Shibli K, et al. Prognostic impact of Notch ligands and receptors in nonsmall cell lung cancer: coexpression of Notch-1 and vascular endothelial growth factor-A predicts poor survival. *Cancer*. 2010;116(24):5676–5685. doi:10.1002/cncr.25551
35. Yuan X, Wu H, Xu H, et al. Meta-analysis reveals the correlation of Notch signaling with non-small cell lung cancer progression and prognosis. *Sci Rep*. 2015;5(1):10338. doi:10.1038/srep10338
36. Yuan X, Wu H, Xu H, et al. Notch signaling: an emerging therapeutic target for cancer treatment. *Cancer Lett*. 2015;369(1):20–27. doi:10.1016/j.canlet.2015.07.048
37. Mohammadi M, Bagheri L, Badreldin A, et al. Biological Effects of Gyrophoric Acid and Other Lichen Derived Metabolites, on Cell Proliferation, Apoptosis and Cell Signaling pathways. *Chem Biol Interact*. 2022;351:109768. doi:10.1016/j.cbi.2021.109768
38. Fagundes R, Teixeira LK. Cyclin E/CDK2: DNA Replication, Replication Stress and Genomic Instability. *Front Cell Dev Biol*. 2021;9:774845. doi:10.3389/fcell.2021.774845
39. Yoshioka KI, Kusumoto-Matsuo R, Matsuno Y, et al. Genomic Instability and Cancer Risk Associated with Erroneous DNA Repair. *Int J Mol Sci*. 2021;23(1):22. doi:10.3390/ijms222212254
40. Klemptner SJ, Fabrizio D, Bane S, et al. Tumor Mutational Burden as a Predictive Biomarker for Response to Immune Checkpoint Inhibitors: a Review of Current Evidence. *Oncologist*. 2020;25:e147–e159. doi:10.1634/theoncologist.2019-0244
41. Bian X, Xiao YT, Wu T, et al. Microvesicles and chemokines in tumor microenvironment: mediators of intercellular communications in tumor progression. *Mol Cancer*. 2019;18(1):50. doi:10.1186/s12943-019-0973-7
42. Suzuki J, Aokage K, Neri S, et al. Relationship between podoplanin-expressing cancer-associated fibroblasts and the immune microenvironment of early lung squamous cell carcinoma. *Lung Cancer*. 2021;153:1–10. doi:10.1016/j.lungcan.2020.12.020
43. Petersen RP, Campa MJ, Sperlazza J, et al. Tumor infiltrating Foxp3 + regulatory T-cells are associated with recurrence in pathologic stage I NSCLC patients. *Cancer*. 2006;107(12):2866–2872. doi:10.1002/cncr.22282

44. Kang DH, Chung C, Sun P, et al. Circulating regulatory T cells predict efficacy and atypical responses in lung cancer patients treated with PD-1/PD-L1 inhibitors. *Cancer Immunol Immunother.* 2022;71(3):579–588. doi:10.1007/s00262-021-03018-y
45. Wang W, Hodkinson P, McLaren F, et al. Small cell lung cancer tumour cells induce regulatory T lymphocytes, and patient survival correlates negatively with FOXP3+ cells in tumour infiltrate. *Int J Cancer.* 2012;131:E928–937. doi:10.1002/ijc.27613
46. Shang B, Liu Y, Jiang SJ, et al. Prognostic value of tumor-infiltrating FoxP3+ regulatory T cells in cancers: a systematic review and meta-analysis. *Sci Rep.* 2015;5(1):15179. doi:10.1038/srep15179
47. Wang X, Xiao Z, Gong J, et al. A prognostic nomogram for lung adenocarcinoma based on immune-infiltrating Treg-related genes: from bench to bedside. *Transl Lung Cancer Res.* 2021;10(1):167–182. doi:10.21037/tlcr-20-822
48. Zhang L, Yi H, Chen J, et al. Neutrophil Extracellular Traps Facilitate A549 Cell Invasion and Migration in a Macrophage-Maintained Inflammatory Microenvironment. *Biomed Res Int.* 2022;2022:8316525. doi:10.1155/2022/8316525
49. Varim C, Celik FD, Sunu C, et al. The role of neutrophil albumin ratio in predicting the stage of non-small cell lung cancer. *Eur Rev Med Pharmacol Sci.* 2022;26:2900–2905. doi:10.26355/eurrev_202204_28621
50. Stares M, Ding TE, Stratton C, et al. Biomarkers of systemic inflammation predict survival with first-line immune checkpoint inhibitors in non-small-cell lung cancer. *ESMO Open.* 2022;7(2):100445. doi:10.1016/j.esmoop.2022.100445
51. Tyagi A, Wu SY, Sharma S, et al. Exosomal miR-4466 from nicotine-activated neutrophils promotes tumor cell stemness and metabolism in lung cancer metastasis. *Oncogene.* 2022;41(22):3079–3092. doi:10.1038/s41388-022-02322-w
52. Zhong R, Chen D, Cao S, et al. Immune cell infiltration features and related marker genes in lung cancer based on single-cell RNA-seq. *Clin Transl Oncol.* 2021;23:405–417. doi:10.1007/s12094-020-02435-2
53. Széles Á, Fazekas T, Váncsa S, et al. Pre-treatment soluble PD-L1 as a predictor of overall survival for immune checkpoint inhibitor therapy: a systematic review and meta-analysis. *Cancer Immunol Immunother.* 2023;72(5):1061–1073. doi:10.1007/s00262-022-03328-9
54. Moran JA, Adams DL, Edelman MJ, et al. Monitoring PD-L1 Expression on Circulating Tumor-Associated Cells in Recurrent Metastatic Non-Small-Cell Lung Carcinoma Predicts Response to Immunotherapy With Radiation Therapy. *JCO Precis Oncol.* 2022;6:e2200457. doi:10.1200/po.22.00457
55. Sánchez-Magraner L, Gumuzio J, Miles J, et al. Functional Engagement of the PD-1/PD-L1 Complex But Not PD-L1 Expression Is Highly Predictive of Patient Response to Immunotherapy in Non-Small-Cell Lung Cancer. *J Clin Oncol.* 2023;41(14):2561–2570. doi:10.1200/jco.22.01748
56. Zhao Y, Ma Y, Zang A, et al. First-in-human Phase I/Ib study of QL1706 (PSB205), a bifunctional PD1/CTLA4 dual blocker, in patients with advanced solid tumors. *J Hematol Oncol.* 2023;16(1):50. doi:10.1186/s13045-023-01445-1

International Journal of General Medicine

Dovepress

Publish your work in this journal

The International Journal of General Medicine is an international, peer-reviewed open-access journal that focuses on general and internal medicine, pathogenesis, epidemiology, diagnosis, monitoring and treatment protocols. The journal is characterized by the rapid reporting of reviews, original research and clinical studies across all disease areas. The manuscript management system is completely online and includes a very quick and fair peer-review system, which is all easy to use. Visit <http://www.dovepress.com/testimonials.php> to read real quotes from published authors.

Submit your manuscript here: <https://www.dovepress.com/international-journal-of-general-medicine-journal>